Mutation in NDUFA13/GRIM19 leads to early onset hypotonia, dyskinesia and sensorial deficiencies, and mitochondrial complex I instability

Claire Angebault Prouteau, Majida Charif, Naig Guegen, Camille Piro-Mégy, Bénédicte Mousson de Camaret, Vincent Procaccio, Pierre-Olivier Guichet, Maxime Hebrard, Gaël Manes, Nicolas Leboucq, et al.

ORIGINAL ARTICLE

Mutation in *NDUFA13/GRIM19* leads to early onset hypotonia, dyskinesia and sensorial deficiencies, and mitochondrial complex I instability

Claire Angebault[1], Majida Charif[1,2], Naig Guegen[2], Camille Piro-Megy[1], Benedicte Mousson de Camaret[3], Vincent Procaccio[2], Pierre-Olivier Guichet[1], Maxime Hebrard[1], Gael Manes[1], Nicolas Leboucq[4], François Rivier[5,6], Christian P. Hamel[1,7], Guy Lenaers[1,2,†] and Agathe Roubertie[1,5,†,*]

[1]Institut des Neurosciences de Montpellier, Université de Montpellier I et II, BP 74103, 34 091 Montpellier Cedex 5, France, [2]Département de Biochimie et Génétique, IBS—CHU Angers, 49933 Angers Cedex 9, France, [3]Maladies Héréditaires du Métabolisme-Pathologies Mitochondriales, Centre de Biochimie et Biologie Moléculaire, 69 677 CHU Bron, France, [4]Service de Neuroradiologie and [5]Service de Neuropédiatrie, CHU Gui de Chauliac, 34 295 Montpellier, France, [6]PhyMedExp, University of Montpellier, INSERM U1046, CNRS UMR 9214, 34295 Montpellier cedex 5, France and [7]Centre of Reference for Genetic Sensory Diseases, 34 295 Montpellier, France

*To whom correspondence should be addressed at: Service de Neuropédiatrie, CHU Gui de Chauliac, 80 Avenue Fliche, 34295 Montpellier, France. Tel: +33 467330182; Fax: +33 467337733; Email: a-roubertie@chu-montpellier.fr

Abstract

Mitochondrial complex I (CI) deficiencies are causing debilitating neurological diseases, among which, the Leber Hereditary Optic Neuropathy and Leigh Syndrome are the most frequent. Here, we describe the first germinal pathogenic mutation in the *NDUFA13/GRIM19* gene encoding a CI subunit, in two sisters with early onset hypotonia, dyskinesia and sensorial deficiencies, including a severe optic neuropathy. Biochemical analysis revealed a drastic decrease in CI enzymatic activity in patient muscle biopsies, and reduction of CI-driven respiration in fibroblasts, while the activities of complex II, III and IV were hardly affected. Western blots disclosed that the abundances of NDUFA13 protein, CI holoenzyme and super complexes were drastically reduced in mitochondrial fractions, a situation that was reproduced by silencing *NDUFA13* in control cells. Thus, we established here a correlation between the first mutation yet identified in the *NDUFA13* gene, which induces CI instability and a severe but slowly evolving clinical presentation affecting the central nervous system.

Introduction

Mitochondrial complex I (CI) or reduced nicotinamide adenine dinucleotide (NADH):ubiquinone oxidoreductase (EC 1.6.5.3) is one of the four enzymes composing the electron transport chain (ETC), which transfers electrons from NADH to ubiquinone, while translocating protons from the matrix to the inner membrane space. CI is a very large complex including two domains, a hydrophilic one located in the matrix and another hydrophobic embedded in the inner membrane; together they require many assembly factors to become an active enzyme (1). CI is composed of 44 subunits, 37 encoded by the nuclear genome (*NDUF* genes, including the NDUFA13 gene) and 7 encoded by the mitochondrial genome (*MTND* genes) (2,3). This holoenzyme

[†]Equal last authors.

is assembled to complex III (CIII) and complex IV (CIV) to form the respirasome supramolecular complex, which represents the most efficient core particle of the ETC (4,5).

CI deficiencies (OMIM 252010) may be caused by nuclear or mitochondrial genome mutations and are the commonest source of mitochondrial disorders, covering a wide spectrum of clinical manifestations ranging from isolated neuro-sensorial diseases in adults to devastating early onset multi-systemic neurological diseases in childhood (6–8). Indeed, some restricted mutations in the mitochondrial *MTND* genes are responsible for the Leber hereditary optic neuropathy (OMIM 535000), a non-syndromic blinding condition due to the degeneration of the retinal ganglion neurons forming the optic nerve (9,10). Alternatively, other *MTND* mutations and mutations in nuclear *NDUF* genes are responsible for early onset severe neuro-developmental disorders, with multiple organ involvement and poor prognosis, exemplified by Leigh syndrome (OMIM 256000). Most diseases associated to CI deficiency are fully ascertained by finding decreased CI-driven respiration and CI enzymatic activity in tissue samples, which are often associated to lactate acidosis in blood, and increased cerebral lactate identified by magnetic resonance spectroscopy (MRS) (1,6,8,11).

To date, 18 nuclear genes and all the 7 mitochondrial *MTND* genes have been involved in inherited diseases with CI deficiency (2,3,7). Here, we report in two sisters with severe hypotonia, dyskinesia and sensorial deficiencies, the first germinal mutation identified in the nuclear *NDUFA13/GRIM19* gene, encoding a peptide required for CI function and stability.

Results

Clinical observations

Patient 1 is the second child born from a consanguineous Turkish couple. Pregnancy and delivery were uneventful, with normal neonatal parameter. Early psychomotor retardation was noticed during the first year; when referred at 13 months, the girl presented axial hypotonia with poor head control, associated to disabling choreoathetoid movements of the limbs and face, while ocular contact and communication were limited. During the following years, abnormal movements progressively improved; she managed to grab objects; pyramidal tract signs worsened progressively. Failure to thrive was noticeable during the first years of life, although feeding difficulties were not reported by the family. At the age of 3.5, abnormal eye movement with slow saccades were noticed; optic disc pallor was diagnosed, and progressed to severe optic atrophy (Fig. 1A); visual acuity could not be evaluated due to her severe mental disability. From the age of 6, the girl exhibited generalized seizures, which were easily controlled by phenobarbital. At the last follow-up at 11.5, the patient was severely handicapped, without occurrence of mental or motor regression; clinical examination showed axial hypotonia, insufficient head control with inability to sit unaided, lower limb spasticity and some degree of global akinesia; she pronounced sounds and, according to the parents, had good interaction with her family members. Weight and height were below the normal range (−1.5 standard deviation), cranial perimeter was normal. No dysmorphic feature was noticed.

Plasmatic and cerebrospinal fluid lactate was normal at 13 months of age, whereas at 10.5 years, plasmatic lactate and alanine were mildly increased to 4.5 mmol/l (normal range <2.5) and to 570 μmol/l (normal range <510), respectively.

Auditory brainstem potential at the age of 5 years disclosed abnormal responses concordant with auditory neuropathy.

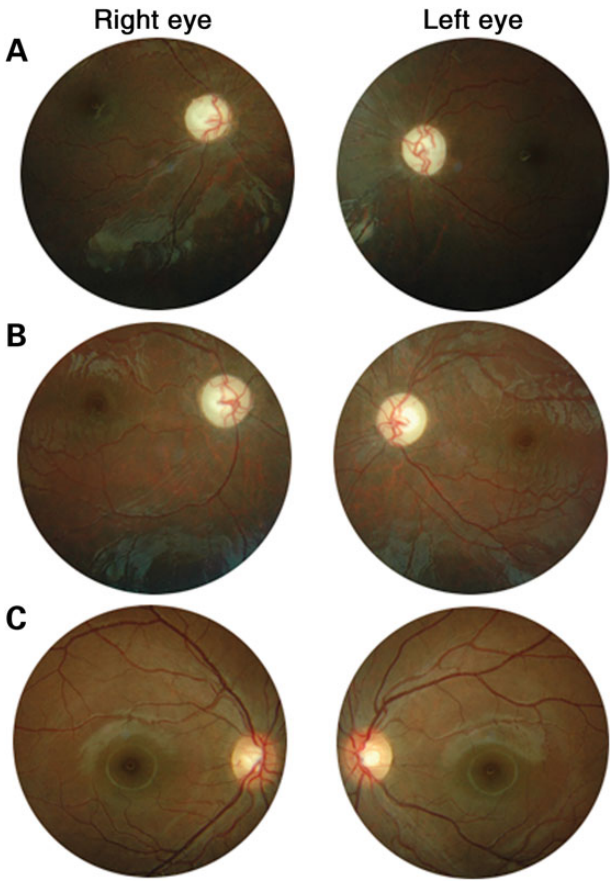

Figure 1. Eye fundus photograph disclosing the optic atrophy. (**A**) Patient 1; (**B**) Patient 2, showing bilateral diffuse advanced optic atrophy characterized by the optic disc pallor. (**C**) Elder unaffected sister, showing normal fundus.

Electroretinogram recording showed subnormal responses. At last follow-up, electromyography recording with conduction velocities, cardiac ultrasound scan and renal function were normal.

Brain magnetic resonance imaging (MRI) performed at 13 months and 3.5 years were normal. At 7 and 10 years, MRI scans showed progressive cerebellar atrophy with hypersignal of the cerebellum and dentate nucleus (Fig. 2A–C); optic nerves were atrophic. MRI spectroscopy showed high lactate peak in the basal ganglia.

Patient 2 is the younger sister of Patient 1. Pregnancy and delivery were uneventful, with normal neonatal parameters. The girl managed to grab at 6 months and sat unaided at 8 months; motor skills poorly progressed thereafter, and she remained stable without regression of her skills. Given a severe gastroesophageal reflux, the patient underwent laparoscopic antireflux surgery at 20 months of age; no feeding troubles were reported afterwards. Abnormal eye movements were noticed at 1 year of age. Funduscopic examination was normal at 18 months, but showed optic atrophy at 5 years of age with a very pale optic disc (Fig. 1B), compared with her non-affected elder sister (Fig. 1C). At 5 years of age, clinical examination disclosed axial hypotonia, with truncal ataxia; pyramidal tract signs were obvious in the lower limbs; she could grab and play with objects despite distal dyskinesia; she was mildly bradykinetic. She was able to repeat syllabus and had good interactions with her family members. Growth parameters were within the

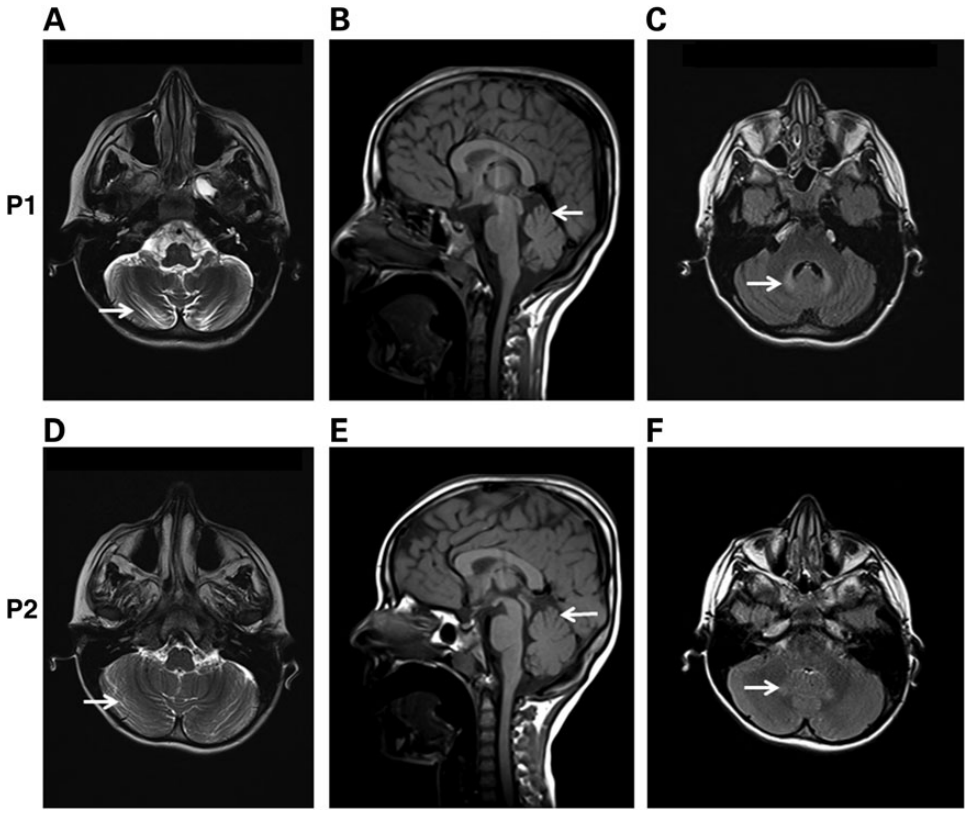

Figure 2. Brain MRI. (**A–C**) Patient 1, aged 10; and (**D–F**): Patient 2, aged 5. (A and D) Axial section T2 sequence revealing showing cerebellar atrophy in Patient 1 (A) and normal cerebellum in Patient 2 (D) (arrows). (B and E) Sagittal section T1 sequence, showing cerebellar atrophy in Patient 1 (B) and normal cerebellum in Patient 2 (E) (arrows). (C and F) Axial fluid attenuated recovery sequence, disclosing hypersignal of the dentate nucleus (arrows).

Table 1. Respiratory complex enzymatic activities (nmoles/min/mg of proteins)

	Complex I	Complex II	Complex III	Complex IV	Citrate synthase
Controls	13.7 (9.8–18.3)	19.3 (13.8–28.0)	118.4 (93.1–139.6)	75.7 (48.5–107.2)	188.4 (103–304)
Patient 1	1.9	9.8	81.5	52.8	174.8
Patient 2	1	11.5	78.2	70.8	245.5

normal range. No dysmorphic feature was noticed. Plasmatic lactic acid dosage at 5 years was increased to 4.1 mmol/l (normal range <2.5).

Auditory brainstem potential performed at 5 years of age disclosed abnormal responses concordant with auditory neuropathy. Electroretinogram recording showed subnormal responses. At last follow-up, electromyography recording with conduction velocities, cardiac ultrasound scan and renal function were normal.

Brain MRI performed at 18 months was normal. At 5 years, MRI scans showed dentate nucleus hyper signal, without cerebellar atrophy (Fig. 2D–F); optic nerves were atrophic. MRI spectroscopy showed high lactate peak in the basal ganglia.

A muscle biopsy was performed on both patients; optic microscopy and histo-enzymologic studies were normal (no ragged-red fibers, normal NADH, SDH and COX enzymatic activities). The respiratory chain enzymes and citrate synthase activities were assayed from isolated mitochondria. CI activity normalized to protein concentration was reduced to 14 and 7% of control values, respectively, in the elder and younger sisters, whereas other complex activities were not significantly affected, or mildly decreased (Table 1).

Molecular and biochemistry investigations

To identify the genetic cause of the disease, we first tested a possible maternal transmission of a heteroplasmic mutation on the mitochondrial genome. The surveyor technique was applied on DNA samples from patient calf muscle, without finding relevant pathogenic mutation. Whole-exome sequencing was then performed on DNA samples from both patients. Progressive filtering of the data revealed 12.702 exonic variants common to both sisters, among which 4.167 were homozygotes and 645 were non-synonymous. Filtering for variants with a frequency lower than 0.003% in the 1600 genes encoding mitochondrial proteins identified three common, homozygote, non-synonymous, damaging, rare variants in the *MFN1*, *C21orf33* and *NDUFA13* genes, the two first being referenced (rs143476739 and rs149515079), whereas the last one was absent from all databases (NCBI, 1000 Genomes and Exome Variant Server). Segregation study in the family by Sanger sequencing excluded the *MFN1* and *C21orf33* mutations. Conversely, it confirmed that the c.G170A mutation in the second exon of the *NDUFA13* gene is homozygote in the two affected sisters, while heterozygote in the parents and the unaffected elder sister (Fig. 3A and B). This mutation

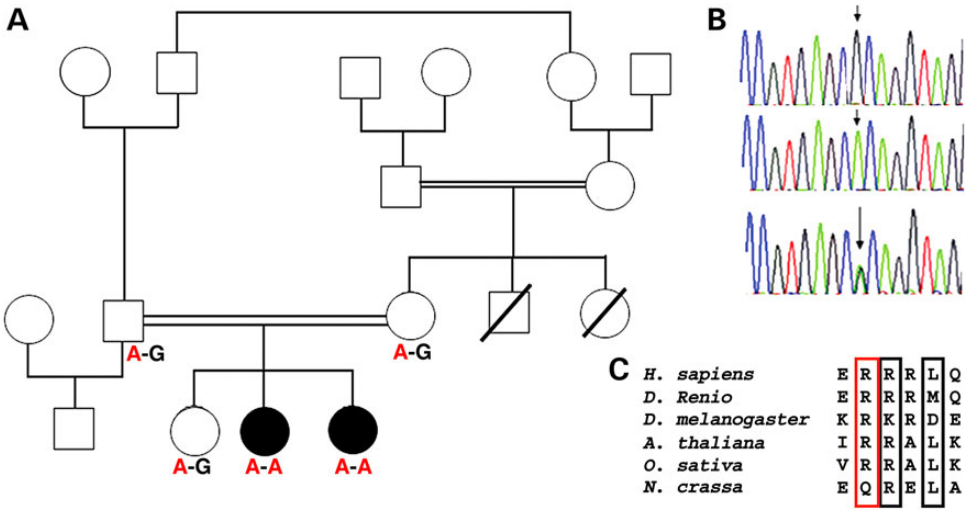

Figure 3. Family pedigree and identification of the mutation in NDUFA13 gene responsible for the clinical presentation. (**A**) The family pedigree shows the different consanguineous marriages and the segregation of the mutation in the close family of the two patients. (**B**) Partial electrophoregram of the Sanger sequencing showing the homozygote, wild-type and heterozygote sequences (arrows). (**C**) Evolutionary conservation of the p.R47 amino acid (squared in red) and conserved neighbor amino acids (squared in black) in eukaryote *NDUFA13* gene sequences from metazoans (human and zebra fish), invertebrates (Drosophila), plants (Arabidopsis and rice) and fungi (Neurospora).

(chr19:19637066) is localized in a 18.7 megabases homozygous region located on chromosome 19p13.1 and changes an arginine strongly conserved among eukaryotes (Fig. 3C) in histidine, p.R57H, a mutation predicted to be damaging and probably damaging by the Sift and Polyphen programs, respectively. Screening of the 5 *NDUFA13* exons in CI deficiency ($n = 44$) cohorts (Leigh syndrome or multi-systemic involvement) or with inherited optic neuropathy ($n = 51$) did not evidence other mutation. This mutation was absent from a control population of 100 unaffected individuals.

To gain insight in the pathogenicity of this novel mutation, we inferred fibroblast primary cultures from skin biopsies of the two patients. Western blots were performed on total protein extracts, using antibodies raised against the NDUFA13, NDUFA9 and NDUFB8 CI proteins, and SDHA from complex II (CII) and β-actin control proteins (Fig. 4A). They revealed a drastic reduction of all CI subunits (mean reduction of 70% for NDUFA13; 95% for NDUFA9 and 90% for NDUFB8) in the two affected sisters, compared with control cells, while no substantial change was observed for the CII and β-actin proteins (Fig. 4B). No difference was observed concerning the quantification of the mRNA of CI in the patients' fibroblasts compared with controls (Supplementary Material, Fig. S1). We then evaluated the integrity of the ETC holoenzymes and supramolecular complexes by running native protein extracts from purified mitochondria on blue-native PAGE (BN PAGE) gels, using antibodies against each respiratory chain complex. In both patient samples, we found a drastic reduction of the abundances of CI and of the supramolecular complex composed of CI, CIII and CIV, whereas that of the other holoenzyme complexes and of the CIII + CIV supramolecular complex remained unchanged (Fig. 4C). In addition, we did not evidence intermediate CI structures, suggesting that the instability of the NDUFA13 protein related to the p.R57H mutation induces a full CI disassembly (Fig. 4D).

We assessed fibroblast CI and CII respiration by oxygraphy and found a mean 40% reduction in CI-related respiration driven by the addition of malate and pyruvate, while that of CII measured in the presence of succinate + rotenone was not altered (Fig. 4E). To ascertain the molecular effects of the *NDUFA13* mutation, we reproduced the drastic decrease in NDUFA13 expression observed in patient fibroblasts, by silencing its expression using siRNA. Evaluation of NDUFA13 abundance was longitudinally followed by western blot and revealed a decrease of 50% (±12%), 24 h after transfection, and of almost 75% after 48 and 72 h (±5 and 21%, respectively) (Fig. 5A and B). Thus, we reconsidered the abundance of CI subunits by western blot, 48 h after the siRNA transfection, and evidenced a drastic reduction of NDUFA9 and NDUFB8 abundances, paralleling that of NDUFA13 (Fig. 5C), as observed in patient fibroblasts and revealing again a major CI instability. We then assessed CI/CII respiration ratio in this experimental condition and found a 33% (±2.6%) reduction of this value compared with control situations, similar to the values we inferred for the two patient fibroblast cultures, thus supporting the pathogenicity of the p.R47H mutation. Finally, we attempted to rescue the biochemical dysfunctions from patient fibroblasts by expressing ectopically *NDUFA13* cDNA. Although the NDUFA13 protein did localize within the mitochondrial network, we observed that NDUFA13 overexpression induced a drastic fragmentation of the mitochondrial network, emphasizing a major alteration of mitochondrial physiology (Supplementary Material, Fig. S2).

Discussion

We have identified here the first germinal mutation in the *NDUFA13* open reading frame in two sisters with a severe neurological presentation. The c.G170A mutation changes the evolutionary conserved p.R57H amino acid that is part of a domain involved in NDUFA13 mitochondrial localization and required for CI assembly. Biochemical and cell biology analyses did not evidence mislocalization of the protein, but they disclosed a high instability of the NDUFA13 protein, that was of major consequence on the stability of other CI subunits, on the full holoenzyme stability and on the constitution of the respirasome complex. Inside CI, NDUFA13 subunit is located in the connecting region between the hydrophobic and the hydrophilic domains and required for their assembly to form the active holoenzyme. Because we have not found CI intermediate structure in

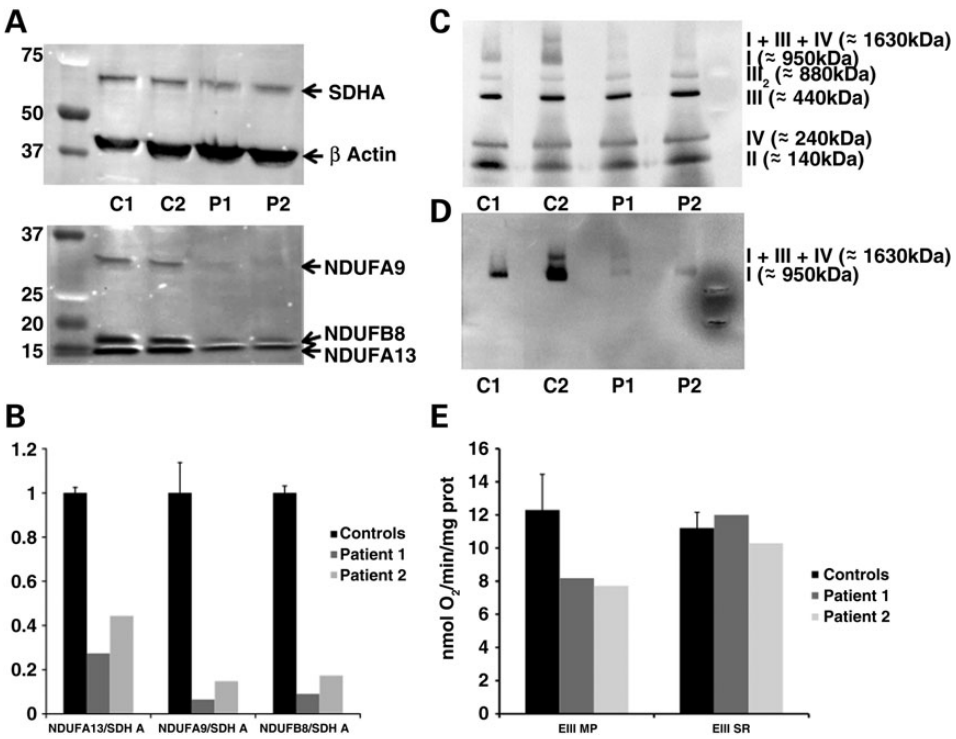

Figure 4. Biochemical assessment of the mitochondrial Complex I characteristics from NDUFA13-mutated fibroblasts. (**A**) Immunoblot analysis on fibroblast protein extracts using NDUFA9, NDUFB8 and NDUFA13 CI and SDHA from CII and β-actin antibodies as controls, showing the drastic decrease of CI subunit abundances. Experiments were performed on five independent control strains (two left bands are representation of the controls) and on the two patient fibroblast lines (right). (**B**) Mean values of the protein abundances assessed by Image-J, from three western blot experiments performed as in (A), for the five controls and the two patients (P1 and P2). Bars indicate the standard errors of the mean values. (**C**) BN PAGE analysis of isolated mitochondria of control (C1 and C2) and patient (P1 and P2) fibroblasts using NDUFA9 and NDUFB6 for CI, SDHA for CII, UQCRC2 for CIII and COX1 for CIV showing the decreased abundances in patients of CI holoenzyme and CI + CIII + CIV supramolecular complex, while the abundances of the CII, CIII and CIV holoenzymes and supramolecular complex CIII + CIV remained unchanged. (**D**) BN PAGE analysis of the same fractions as in **C** probed with the NDUFA9 and NDUFB6 antibodies, showing the decreased abundance of CI holoenzyme and the absence of intermediate CI structure. (**E**) Oxygen consumption analyzed by oxygraphy in three control fibroblasts and the two patient fibroblasts. EIII MP and EIII SR indicate the respiration driven by the CI in the presence of malate + pyruvate, and the respiration driven by the CII in the presence of succinate and rotenone, respectively. Bars indicate the standard errors of the means between the control samples.

mitochondria purified from the patient fibroblasts, we hypothesized that the p.R47H mutation and the reduction of NDUFA13 abundance affect drastically CI stability, and consequently its enzymatic activity in patient muscle biopsies, as well as the CI-driven respiration in fibroblasts.

Somatic mutations in a *NDUFA13* alternate open reading frame have been identified in samples of Hurthle carcinoma cells, a rare form of thyroid cancer showing increased mitochondrial number (4,5,12). These somatic mutations were all heterozygous and affected the N-terminal sequence of long NDUFA13 isoform, whereas the mutation found here was homozygous and affected the short isoform. Nevertheless, we have not found any sign of mitochondrial proliferation in our samples, neither by cell biology (not shown) nor by biochemical assessments, as the citrate synthase activity and the quantity of CII, CIII and CIV subunits were all in normal ranges. *NDUFA13* gene has also been identified as the 19th gene associated with retinoid and interferon-induced mortality (*GRIM19*) (6–8,13,14), suggesting an additional function for the NDUFA13 protein unrelated to CI assembly and activity. This hypothesis is reinforced by additional results disclosing interactions between NDUFA13 and viral Kaposi and papillomavirus proteins (9,10,15), and with the transcription factor STAT3 (16), resulting in the inhibition of the cell cycle progression and antioncogenic effects (17). Eventually, the alteration of these functions by the p.R47H mutation could, in addition to the pathogenic CI deficiency, lead to an antiapoptotic effect, which would somehow protect neurons from degeneration and explain the slow evolution of the disease. Thus the contribution of the somatic *NDUFA13* mutations to the Hurthle cancer are most probably related to a process different from the etiology caused by the germinal p.R47H mutation, causing the neurological presentation described here. Nevertheless the broad range of NDUFA13 functions could contribute to the specificity of this clinical presentation, which is different from the classical severe neurological diseases caused by CI deficiency, as Leigh syndrome, although the variability of clinical phenotypes associated to isolated CI deficiency increases monthly (6–8).

Indeed, our patients presented an infantile-onset slowly progressive encephalopathy, with axial hypotonia, dyskinesia, hearing loss, severe optic neuropathy with retinal dysfunction, pyramidal tract signs and lactic acidosis, without extra-neurological involvement. This clinical presentation is concordant with a CI deficiency. Nevertheless our patients are singular by the very slow rate of progression of their neurological symptoms despite the very young age at onset of the disease. In this respect, their prolonged survival is noteworthy, the elder sister being now 12 years old. Actually, prognosis for patients with nuclear CI deficiency is correlated to the age of onset, with half of the patients dying before 2 years of age, and two-third before 10 years of age (2,7,8). This slow clinical evolution is also consistent with the fact that the *NDUFA13* patients only displayed abnormalities of brain MRI and spectroscopy many years after the onset of the disease. Importantly, imaging characteristic of Leigh syndrome with bilateral and symmetrical abnormal signals

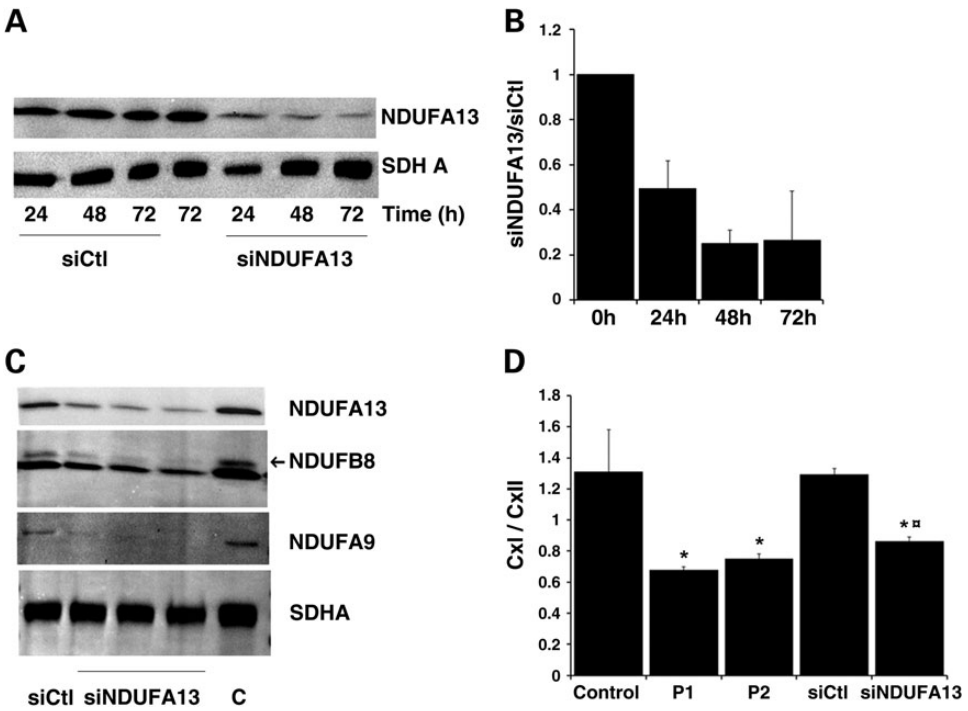

Figure 5. Complex I biochemical assessment associated to NDUFA13 silencing in control fibroblasts. (**A**) Immunoblot analysis on protein extracts from fibroblasts transfected with NDUFA13 siRNA (siNDUFA13, right), control siRNA (siCtl, left) or lipofectamine only (C) showing the decrease of NDUFA13 abundances after 24, 48 and 72 h. SDHA from CII was used as a mitochondrial loading control. Experiments were performed on three independent transfection experiments. (**B**) Mean values of the protein abundances assessed by Image J, from three western blot experiments performed as in (A). Bars indicate the standard errors of the mean values. (**C**) Protein extracts were performed on three independent cultures transfected with the NDUFA13 siRNA (siNDUFA13, middle), one with the control siRNA (siCtl) and one untransfected (C). Immunoblots performed using the NDUFA9, NDUFB8 and NDUFA13 CI antibodies and the SDHA CII antibodies reveal the drastic decrease of CI subunit abundances. (**D**) Fibroblast oxygen consumption analyzed by oxygraphy, 48 h after control (siCtl) and NDUFA13 (siNDUFA13) siRNA transfections, and compared with control and NDUFA13 patient (P1 and P2) fibroblasts. EIII MP (CxI) and EIII SR (CxII) indicate the respiration driven by the CI in the presence of malate + pyruvate, and the respiration driven by the CII in the presence of succinate and rotenone, respectively. Bars indicate the standard errors of the mean values. * $P < 0.05$ compared with control fibroblasts $^{\square}P < 0.05$ compared with siRNA control.

of the basal ganglia (4,5,18) was not observed here, but the abnormal signal intensities in brainstem and subtentorial nuclei, and the lactate peak reported for the two sisters are concordant with similar common patterns identified in a recent study of 30 patients with CI deficiency (6–8,11).

It is often a challenge for the clinician to establish the molecular diagnosis of a patient with CI deficiency. Some authors tried to draw phenotype–genotype correlations in order to orientate the genetic diagnosis; for example it was suggested that the observation of cerebellar atrophy should prompt the screening of *MTND* genes from the mitochondrial genome instead of *NDUF* genes from the nuclear genome (9–11). In the light of our observations, this paradigm at least can be re-evaluated, as we found a cerebellar atrophy in the elder sister with the *NDUFA13* mutation. Therefore, and given the growing number of gene mutated in CI patients and the diversity of the clinical presentations, it becomes more and more evident that routinely sequencing all the CI genes from the nucleus and mitochondrial genomes, using targeted captures of their open reading frames, will provide the clinician with exhaustive and pertinent genetic information to complete the clinical and biochemical diagnoses of CI-related diseases.

Materials and Methods

Informed consents were obtained from the parents to perform genetic, biochemical and molecular analyses and to publish all data.

Molecular biology

To identify the pathogenic mutation in the two affected sisters, we performed whole-exome sequencing, using SureSelect Human All Exon Kits Version 3 methodology (Agilent, Santa Clara, CA), followed by high-throughput sequencing. Data were filtered for common homozygote non-synonymous mutations in gene encoding mitochondrial protein, with an occurrence lower than 1 in 300 in the exome variant server database. The mutation in *NDUFA13* gene was confirmed and its familial segregation established by Sanger sequencing. Informed consents were obtained from the patients and their parents to perform clinical, biochemical and genetic analysis.

Enzymatic measurements on skeletal muscle

Vastus lateralis muscle biopsies were taken by the percutaneous Bergström technique after local anesthesia (Xylocaine). ETC complex activities were measured from a 800 g supernatant of crude muscle homogenates as described (17,19).

Oxygen consumption

Respiration was measured on fibroblasts permeabilized by incubation for 2 min with 15 µg digitonin per million cells and resuspended in the respiratory buffer (pH 7.4, 10 mM KH_2PO_4, 300 mM mannitol, 10 mM KCl and 5 mM $MgCl_2$). The respiratory rates of $3–5 \times 10^6$ cells were recorded at 37°C in 2 ml glass chambers

using a high-resolution Oxygraph respirometer (Oroboros, Innsbruck, Austria). Respiration was started with complex I-dependent substrates (5 mM malate/5 mM pyruvate). Complex I-coupled state 3 respiration was measured by adding 0.5 mM NAD^+/1.5 mM ADP. Then, 10 mM succinate was added to reach maximal coupled respiration, and 10 µM rotenone were injected to obtain the CII-coupled state 3 respiration. Oligomycin (8 µg/ml) was added to determine the uncoupled state 4 respiration. Finally, carbonyl cyanide-4-(trifluoromethoxy) phenylhydrazone (1 µM) was added to control the permeabilization of the fibroblasts.

Western blot analysis

Frozen cell pellets were lysated by a hypo-osmotic shock (10 µl $H_2O/10^6$ cells) and the cellular protein content was determined with the Bicinchoninic assay kit. Twenty micrograms of total protein were separated on a 10% SDS-polyacrylamide gel and electro-blotted onto a PVDF membrane (Bio Rad). Membranes were saturated with 5% non-fat milk dissolved in TBS-Tween 0.1% (pH 7.4, NaCl 137 mM, KCl 2.7 mM, Tris 23 mM, Tween 0.1%) for 1 h at room temperature and incubated overnight at 4°C with monoclonal mouse anti-NDUFB8 (1/2.000 Mitosciences), anti-NDUFA9 (1/1 000 Mitosciences), anti-NDUFA13 (1/1.000 Mitosciences), anti-SDH A (1/1.000 Mitosciences) and anti-actin (1/1.000 Sigma). Membranes were then washed three times in TBS-Tween 0.1% and incubated with anti-mouse IgG horseradish peroxidase linked antibody (1/10 000 Sigma) for 1 h at room temperature. The immunoreactive proteins were visualized with enhanced chemiluminescence (ECL + Western Blotting Detection Reagents, Amersham Biosciences). Band intensities were quantified with Image J.

BN PAGE

Mitochondria-enriched extracts were obtained from fibroblasts by differential centrifugation and resuspended at 5 mg/mL in 1.5 M 6-aminocaproïc acid, 75 mM Bis-Tris at pH 7.0 and antiprotease (Roche). *N*-dodecyl-β-D-maltopyranoside (3 g/g of mitochondrial protein) was added for 10 min to obtained complex in monomeric form and supercomplex assembly. After 20 min of centrifugation at 10 000*g*, the supernatant was collected and added to the loading buffer (Coomasie brilliant blue G 250 5%, 6-aminocaproïc acid 750 mM, EDTA 0.5 mM and Bis Tris 50 mM at pH 7.0). Forty micrograms of proteins were loaded on BN PAGE 3–12% Bis-Tris gel (Invitrogen) and separated at 150 V. Following transfer to membranes (Amersham) and saturation with 10% in non-fat milk dissolved in TBS-Tween 0.1%, the presence of complex I, II, III and IV were assessed using antibodies against NDUFA9 and NDUFB6, SDHA, III core 2 and COX I, respectively (Mitosciences) and revealed by anti-mouse IgG horseradish peroxidase linked antibody (1/10 000 Sigma) as described for western blots.

siRNA and transfection

Control fibroblast cells were transfected with siRNA directed against NDUFA13 (Thermo Fisher Scientific Biosciences, ON-TARGET plus Human NDUFA13 (51079) siRNA SMART pool) with Lipofectamine 2000 (Invitrogen) according to manufacturer's instructions and processed 48 h later for western blot or oxygraphy analyses.

Statistical analysis

The non-parametric Mann–Whitney *U*-test was used to compare the fibroblasts from NDUFA13 patients, to fibroblasts transfected with siRNA and controls. Differences were considered significant at $P < 0.05$ (* and °).

Database references

The *NDUFA13* gene, located on chromosome 19p13.11, is referenced as *609435 in NCBI and as NG_013380.1 in the LOVD database, its mRNA is referenced as NM_015965.6 in NCBI or ENSP00000423673 in Ensembl and the 144 amino-acid protein is referenced as AAH09189 in NCBI and CCDS12404 in Ensembl.

The accession number of the NDUFA13 variant is SCV000153676 (URL: http://www.ncbi.nlm.nih.gov/clinvar/?term=SCV000153676).

Supplementary Material

Supplementary Material is available at *HMG* online.

Acknowledgements

We are indebted to the INSERM and its Pôle Relations Internationales—DPRE, the CNRS, the University Montpellier I and II for institutional support and providing a traveling INSERM/CNRST grant to M.C. We are indebted to Dr Lagavulin and colleagues from the Institut des Neurosciences de Montpellier for generating helpful discussions.

Conflict of Interest statement. All authors declare that they do not have conflict of interest or private interest in publishing this manuscript.

Funding

We acknowledge the financial support from the Agence Nationale de la Recherche, Genzyme, and from Retina France, UNADEV and Ouvrir Les Yeux patient associations.

References

1. Lazarou, M., Thorburn, D.R., Ryan, M.T. and McKenzie, M. (2009) Assembly of mitochondrial complex I and defects in disease. *Biochim. Biophys. Acta*, **1793**, 78–88.
2. Balsa, E., Marco, R., Perales-Clemente, E., Szklarczyk, R., Calvo, E., Landázuri, M.O. and Enriquez, J.A. (2012) NDUFA4 is a subunit of complex IV of the mammalian electron transport chain. *Cell Metab.*, **16**, 378–386.
3. Hoefs, S.J.G., Rodenburg, R.J., Smeitink, J.A.M. and van den Heuvel, L.P. (2012) Molecular base of biochemical complex I deficiency. *Mitochondrion*, **12**, 520–532.
4. Acín-Pérez, R., Fernández-Silva, P., Peleato, M.L., Pérez-Martos, A. and Enriquez, J.A. (2008) Respiratory active mitochondrial supercomplexes. *Mol. Cell*, **32**, 529–539.
5. Vonck, J. and Schäfer, E. (2009) Supramolecular organization of protein complexes in the mitochondrial inner membrane. *Biochim. Biophys. Acta*, **1793**, 117–124.
6. Distelmaier, F., Koopman, W.J.H., van den Heuvel, L.P., Rodenburg, R.J., Mayatepek, E., Willems, P.H.G.M. and Smeitink, J.A.M. (2008) Mitochondrial complex I deficiency: from organelle dysfunction to clinical disease. *Brain*, **132**, 833–842.
7. Fassone, E. and Rahman, S. (2012) Complex I deficiency: clinical features, biochemistry and molecular genetics. *J. Med. Genet.*, **49**, 578–590.
8. Koene, S., Rodenburg, R.J., Knaap, M.S., Willemsen, M.A.A.P., Sperl, W., Laugel, V., Ostergaard, E., Tarnopolsky, M., Martin, M.A., Nesbitt, V. *et al.* (2012) Natural disease course and

genotype–phenotype correlations in Complex I deficiency caused by nuclear gene defects: what we learned from 130 cases. *J. Inherit. Metab. Dis.*, **35**, 737–747.
9. Wallace, D.C., Singh, G., Lott, M.T., Hodge, J.A., Schurr, T.G., Lezza, A.M., Elsas, L.J. and Nikoskelainen, E.K. (1988) Mitochondrial DNA mutation associated with Leber's hereditary optic neuropathy. *Science*, **242**, 1427–1430.
10. Carelli, V., Ross-Cisneros, F.N. and Sadun, A.A. (2004) Mitochondrial dysfunction as a cause of optic neuropathies. *Prog. Retin. Eye Res.*, **23**, 53–89.
11. Lebre, A.S., Rio, M., Faivre d'Arcier, L., Vernerey, D., Landrieu, P., Slama, A., Jardel, C., Laforet, P., Rodriguez, D., Dorison, N. *et al.* (2010) A common pattern of brain MRI imaging in mitochondrial diseases with complex I deficiency. *J. Med. Genet.*, **48**, 16–23.
12. Moreira, S., Correia, M., Soares, P. and Máximo, V. (2011) GRIM-19 function in cancer development. *Mitochondrion*, **11**, 693–699.
13. Hofmann, E.R., Boyanapalli, M., Lindner, D.J., Weihua, X., Hassel, B.A., Jagus, R., Gutierrez, P.L., Kalvakolanu, D.V. and Hofman, E.R. (1998) Thioredoxin reductase mediates cell death effects of the combination of beta interferon and retinoic acid. *Mol. Cell. Biol.*, **18**, 6493–6504.
14. Huang, G., Lu, H., Hao, A., Ng, D.C.H., Ponniah, S., Guo, K., Lufei, C., Zeng, Q. and Cao, X. (2004) GRIM-19, a cell death regulatory protein, is essential for assembly and function of mitochondrial complex I. *Mol. Cell. Biol.*, **24**, 8447–8456.
15. Seo, T., Lee, D., Shim, Y.S., Angell, J.E., Chidambaram, N.V., Kalvakolanu, D.V. and Choe, J. (2002) Viral interferon regulatory factor 1 of Kaposi's sarcoma-associated herpesvirus interacts with a cell death regulator, GRIM19, and inhibits interferon/retinoic acid-induced cell death. *J. Virol.*, **76**, 8797–8807.
16. Zhang, J., Yang, J., Roy, S.K., Tininini, S., Hu, J., Bromberg, J.F., Poli, V., Stark, G.R. and Kalvakolanu, D.V. (2003) The cell death regulator GRIM-19 is an inhibitor of signal transducer and activator of transcription 3. *Proc. Natl. Acad. Sci. USA*, **100**, 9342–9347.
17. Tammineni, P., Anugula, C., Mohammed, F., Anjaneyulu, M., Larner, A.C. and Sepuri, N.B.V. (2013) The import of the transcription factor STAT3 into mitochondria depends on GRIM-19, a component of the electron transport chain. *J. Biol. Chem.*, **288**, 4723–4732.
18. Rahman, S., Blok, R.B., Dahl, H.H., Danks, D.M., Kirby, D.M., Chow, C.W., Christodoulou, J. and Thorburn, D.R. (1996) Leigh syndrome: clinical features and biochemical and DNA abnormalities. *Ann. Neurol.*, **39**, 343–351.
19. Medja, F., Allouche, S., Frachon, P., Jardel, C., Malgat, M., Mousson de Camaret, B., Slama, A., Lunardi, J., Mazat, J.P. and Lombès, A. (2009) Development and implementation of standardized respiratory chain spectrophotometric assays for clinical diagnosis. *Mitochondrion*, **9**, 331–339.